What Affects the Quartet−Doublet Energy Splitting in Peroxidase Enzymes?

Sam P. de Visser*

School of Chemical Engineering and Analytical Science, The University of Manchester, Sackville Street, P.O. Box 88, Manchester M60 1QD, United Kingdom

Received: July 14, 2005; In Final Form: September 30, 2005

Density functional theory calculations have been performed on the active species (Compound I) of cytochrome *c* peroxidase (C*c*P) and ascorbate peroxidase (APX) models. We have calculated a large model containing oxo−iron porphyrin plus a hydrogen-bonded network of the axial bound imidazole ligand connected to an acetic acid and an indole group, which mimic the His_{175}, Asp_{235}, and Trp_{191} amino acids in cytochrome *c* peroxidase. Our optimized geometries are in good agreement with X-ray and crystallographic structures and give an electronic ground state in agreement with EPR and ENDOR results. We show that the quartet−doublet state ordering and the charge distribution within the model are dependent on small external perturbations. In particular, a single point charge at a distance of 8.7 Å is shown to cause delocalization of the charge and radical characters within the model, thereby creating either a pure porphyrin cation radical state or a tryptophan cation radical state. Thus, our calculations show that small external perturbations are sufficient to change the electronic state of the active species and subsequently its catalytic properties. Similar effects are possible with the addition of an electric field strength along a specific coordination axis of the system. The differences between the electronic ground states of C*c*P and APX Cpd I are analyzed on the basis of external perturbations.

Introduction

Heme-type enzymes appear in many different biosystems and are involved in oxygen transport as well as monoxygenation processes.[1,2] One of the first heme enzymes of which the active species (Compound I, Cpd I) was characterized is cytochrome *c* peroxidase (C*c*P); as such, it has been the topic of many scientific studies.[3−5] The major function of the enzyme is to reduce hydrogen peroxide to water.[4] Structurally, the active center of the enzyme contains an iron atom embedded into a heme group that is bound to two more ligands.[3] One of these is the axial ligand and is the connection of the iron-heme group with the protein backbone. In the case of peroxidases, such as C*c*P or horseradish peroxidase (HRP), this axial ligand is the imidazole side chain of a histidine residue, while in chloroperoxidase (CPO) it is a thiolate of a cysteinate residue.[6−8] It was shown that the nature of this axial ligand creates either a push or a pull effect on the iron center that influences its catalytic properties.[9,10] The sixth ligand bound to iron is an exchangeable moiety; in the resting state, it is a water molecule. Upon hydrogen peroxide binding, the water molecule is displaced and the catalytic cycle starts, thereby converting the iron−hydrogen peroxide into iron−oxo (Fe^{V}═O) and water.[11] For many years, C*c*P was considered as the benchmark peroxidase model; however, unlike other peroxidase systems, the electronic ground state of Cpd I is quite different, namely, that it contains a protein radical rather than a heme radical. Typically, peroxidases have a Cpd I state with close-lying quartet and doublet spin states, both containing a triradicaloid system with two unpaired electrons in π^*_{FeO} orbitals coupled to a third unpaired electron located in a nonbonding heme orbital with a_{2u} symmetry.[12,13] Since the coupling between the π^*_{FeO} orbitals and the a_{2u} orbital is small, the ferromagnetic quartet and antiferromagnetic doublet states are close in energy. Instead of an unpaired electron in the heme a_{2u} molecular orbital, it was found that C*c*P has a radical located on a nearby tryptophan residue (Trp_{191}) as identified by EPR and ENDOR studies.[14,15] Many studies have been performed to identify the nature of the protein radical in C*c*P Cpd I, but until now no answer is conclusive.

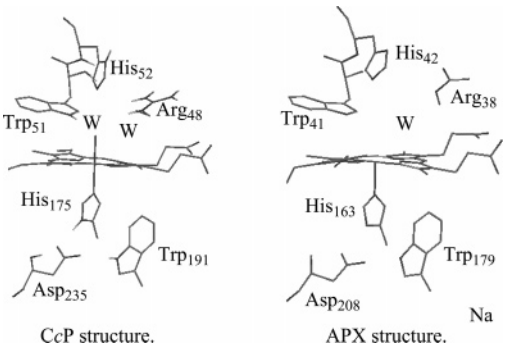

Figure 1. X-ray structures of the resting states of C*c*P (left) and APX (right) as taken from the 1CCA[6] and 1OAF[16] pdb files of the Protein Data Bank.[18] Characteristic amino acid groups have been identified and are labeled as in the X-ray structures. Water molecules are identified with W.

An enzyme related to C*c*P is ascorbate peroxidase (APX) that has an analogous structure and an almost identical active site.[16,17] Figure 1 displays the active sites of the resting states of these two enzymes side-by-side with labels from the pdb structures.[6,16,18] The resting state contains a water molecule bound to the sixth coordination site of the enzyme. As can be seen, structurally the active sites of C*c*P and APX are almost identical, since they contain the same amino acid residues in roughly the same position. The three amino acid groups depicted in the distal site are the tryptophan, histidine, and arginine residues, which are involved in the protonation machinery to convert hydrogen peroxide into water. The axial site contains a

* Tel: +44-161-3064882. Fax: +44-161-3064399. E-mail: sam.devisser@manchester.ac.uk.

10.1021/jp053873u CCC: $30.25
Published on Web 11/10/2005

triad of hydrogen-bonded amino acids: histidine, aspartate, and tryptophan residues. These axial groups fine-tune the redox potential of the metal, and their push or pull effects determine the nature of the iron center.[9] The only difference between the C*c*P and APX active sites appears to be a cation binding site, occupied by a Na^+ ion in APX, in the axial region at approximately 8.7 Å from Trp_{179}. Thus, it was shown that engineering the C*c*P structure with a cationic binding loop containing a K^+ ion gave destabilization of the tryptophan radical although the formation of the tryptophan radical was not altered.[19]

Subsequent mutations in this hydrogen-bonded triad and the effects this has on the properties of the enzyme were studied.[6] In particular, mutation of Asp_{235} to glutamic acid showed retention of most of the structure and an activity similar to that of the wild-type enzyme. However, disruption of the hydrogen-bonded triad by mutation of Asp_{235} by either glycine or alanine resulted in major structural changes and activity loss. Especially, in these mutants the tryptophan residue moved away from its original position to form a new hydrogen bond with a Leu_{177} group. These mutations also strongly affected the reduction potentials of the active species due to the fact that the axial ligand histidine was not protonated in the mutants.[6] Further mutations with the axial histidine amino acid replaced by glycine (H175G) and the addition of imidazole gave imidazole as axial ligand instead of histidine. Although it was found that imidazole (ImH) is a weaker ligand than histidine, most of the hydrogen-bonded interactions, such as the hydrogen-bonded triad (ImH-Asp_{235}-Trp_{191}), stayed intact and the ability of the mutant to react with hydrogen peroxide was more or less retained although the oxidation process was found to be inefficient.[20,21] Electronically, the H175G mutant with axial imidazole bound was found to be in an antiferromagnetically coupled doublet ground state, whereas the wild-type enzyme has a ferromagnetically coupled quartet ground state.[21] Thus, seemingly small changes to the structure of the enzyme may lead to large electronic differences and sometimes even to reversal of the quartet−doublet energy gaps.

In the past, many theoretical studies have been performed on peroxidase model systems.[12,13,22−25] The smallest models studied oxo−iron porphyrin with an imidazole group for the histidine axial ligand. Major conclusions from these studies were that the imidazole side chain of His_{175} is likely to be protonated since calculations on a peroxidase model with imidazole (ImH) reproduced experimental quartet−doublet splittings, whereas imidazolate (Im^-) did not.[12] Moreover, with imidazole as an axial ligand, specific spectroscopic features could be reproduced.[13]

One specific study orientated around the electronic properties of Cpd I of C*c*P and included a large model which apart from oxo−iron porphyrin also included an imidazole group replacing His_{175}, a formate ion in the place of Asp_{235}, and an indole group for Trp_{191}.[24] Only the quartet spin state was studied, but it was shown that although it was expected that the radical should be located on the indole group there still was partial spin density found on the heme ($\rho_{porphyrin} = 0.48$; $\rho_{indole} = 0.47$). It was ascertained that this mixing of porphyrin radical with indole radical was the result of close-lying ionization energies of these two groups. Several protonation states within the hydrogen-bonded triad His_{172}-Asp_{235}-Trp_{191} were tested, and the most stable configuration contained a deprotonated aspartate group.

Other theoretical studies of Warshel et al.[22] used the Langevin dipoles method to calculate the redox potentials of C*c*P and APX. Their calculations showed that the axial tryptophan residue in APX is 330 mV more difficult to oxidize than the related tryptophan group in C*c*P. Part of this was attributed to the K^+ binding site in APX, but in fact it was the sum of a series of smaller contributions rather than one major specific effect.

Therefore, heme enzymes such as peroxidases seem to be able to change their electron affinity due to small perturbations, some local and others nonlocal. Since heme enzymes possess close-lying doublet and quartet spin states, it is the environmental factors that determine which of these is the ground state.[2] Although the doublet and quartet spin states of Cpd I have the same orbital occupation, their reactivity patterns can be quite different.[13] Specifically, substrate oxidation by Cpd I occurs via competing reaction processes on the two spin state surfaces, that is, there are doublet and quartet reaction mechanisms. This process has been termed two-state reactivity and appears to be general in oxo−iron porphyrin systems.[26] In the past we calculated many different reaction mechanisms of P450 models and found several examples whereby the doublet and quartet reaction mechanisms were different.[27−31] In particular, on the doublet spin surface, alkene epoxidation occurs via a concerted mechanism; however, on the quartet spin surface, the process is stepwise.[27−29] Thus, a stepwise mechanism creates an intermediate complex with a finite lifetime, which may rearrange and create (unwanted) side-products. For instance, it was shown that intermediates in the epoxidation reaction on the quartet spin surface can rearrange to form suicidal complexes or aldehyde products, whereas these processes are not accessible on the doublet spin surface.[27] Consequently, in the case of alkene epoxidation reactions by P450 enzymes, the doublet spin mechanism is stereospecific, whereas the quartet spin mechanism is not. Other reactions carried out by P450 enzymes, such as the hydroxylation of *trans*-methyl phenyl cyclopropane, were also studied and these calculations showed that on the doublet spin surface rearrangement is unlikely, whereas it is dominant on the high-spin surface.[30] As a consequence the two processes give a product isotope effect, which was matched with experimental data. In other work, it was shown that the sulfoxidation reaction as catalyzed by P450 enzymes is dominant on the high-spin (quartet) surface, in contrast to benzene hydroxylation which is dominant on the low-spin (doublet) surface.[31] These reactivity studies show that the doublet−quartet energy gap is an important feature of heme enzymes, since it can influence the reactivity and catalysis of substrates as well as the product distribution.

In this paper we present a detailed study of the active species of cytochrome *c* peroxidase and the ordering of the low-lying electronic states as a function of external perturbations. We will show that the quartet−doublet splitting in peroxidase model systems is dependent on local electrostatic interactions, such as a point charge. Furthermore, the quartet−doublet energy gap can be fine-tuned by specific interactions of the active center residues with its surroundings.

Methods

All structures as described here were fully optimized using the Jaguar 5.5 program package[32] using previously described procedures.[25] We use the unrestricted hybrid density functional method UB3LYP[33,34] in combination with an LACVP basis set.[35] This basis set essentially uses an LACVP double ζ quality basis set on iron and a 6-31G basis set on all other atoms. Subsequently, an analytical frequency using the Gaussian-98 package[36] confirmed that the structures discussed here were local minima with real frequencies only. Thereafter, single point calculations with the LACV3P+* basis set[35] using the triple ζ

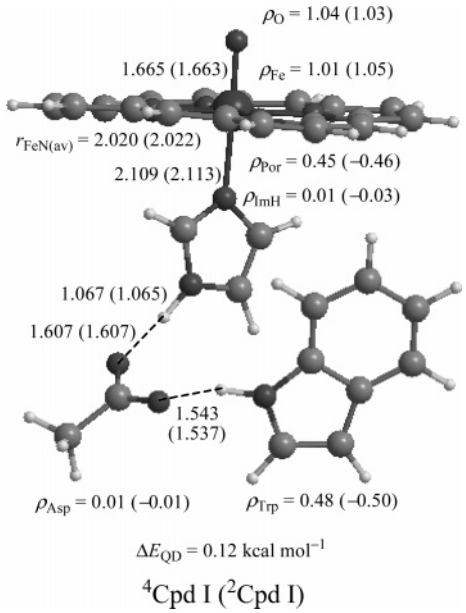

Figure 2. Optimized UB3LYP/LACVP geometries of ^{4}Cpd I (^{2}Cpd I) using a large model in Jaguar. Bond lengths are in angstroms. Also shown are group spin densities as obtained from the Gaussian frequency calculation.

quality LACV3P basis set on iron and a 6-311+G* basis set on the rest of the atoms were performed.

As a model for the active site of cytochrome *c* peroxidase Compound I (C*c*P Cpd I), we used the coordinates of the crystal structure of Goodin and McRee.[6] We limited our model to oxo−iron porphine with imidazole replacing the His_{175} axial ligand and acetic acid and indole replacing the axial amino acid side chains of Asp_{235} and Trp_{191} as these three amino acids form a hydrogen-bonded triad.[6] The overall charge of this system is zero, and the spin multiplicities tested by us were the doublet and quartet spin states. In the following, HS stands for high-spin (quartet) and LS for low-spin (doublet).

To model the effect of the environment on the ordering of the low-lying electronic states, we tested two typical dielectric constants, $\epsilon = 5.7$ and $\epsilon = 10.65$, mimicking the dielectric constant range in these type of enzymes. These calculations were performed with the Jaguar 5.5 program package[32] and used a probe radius of 2.72 and 2.51 Å, respectively. On the basis of earlier work, we also tested the effect of an applied electric field on the low-lying electronic states of Cpd I following previously reported procedures.[37]

The two closely related enzymes APX and C*c*P have similar active sites but differ due to a cation binding site in APX. Thus, to test differences between these two enzymes we tested the effect of a point charge on the nature of the electronic ground states by placement of this point charge exactly in the position of the ion in the X-ray structure with respect to the heme group as taken from the 1OAF pdb.[16] Single point calculations using the UB3LYP/LACVP method in Gaussian-98 gave the corresponding relative energies and charge distribution.

Results

Figure 2 shows the optimized geometries of the lowest-lying quartet and doublet spin states of our model of cytochrome *c* peroxidase (C*c*P) Cpd I. Also shown is the energy difference between the lowest quartet and doublet spin states of 0.12 kcal mol^{-1} in favor of the quartet. The system is characterized by short Fe−O distances reflecting the double bond between the two atoms and are 1.665 and 1.663 Å in the HS and LS spin states, respectively. These values are in line with the X-ray data of Chance et al.[38] on C*c*P Cpd I, who obtained a value of 1.67 Å, and with DFT calculations on a smaller quartet spin state model of C*c*P Cpd I where a value of 1.657 Å was calculated.[24] Our calculated Fe═O bond distances are somewhat longer than the ones obtained for a small peroxidase system with either only an imidazole axial ligand or with an extra formate anion hydrogen-bonded to imidazole. With these models, Fe═O distances of 1.621−1.625 Å were obtained.[25]

The axial ligand (histidine) is bound by a relatively long Fe−N bond of 2.109 (2.113) Å in the HS (LS) spin states, which is in good agreement with distances obtained for the resting state of C*c*P of 2.10 and 2.0 Å, while for HRP Cpd I a value of 2.1 Å was obtained.[3,7,39] Previous work on smaller peroxidase models gave Fe−N_{ImH} distances of 2.173 (2.175) Å for a model containing only imidazole, whereas a model with a hydrogen-bonded formate ion gave distances of 2.158 (2.160) Å in the HS (LS) spin states.[25] Thus, a hydrogen-bonding interaction toward the axial histidine group shortens the Fe−N_{ImH} distance slightly, and further extension of the hydrogen-bonded network with the corresponding tryptophan residue as shown here in Figure 2 shortens the Fe−N_{ImH} distance even further. Therefore, hydrogen-bonding interactions toward the imidazole axial ligand increase the strength of the Fe−N_{His} bond and as a result will influence the electron affinity and electronic properties of the catalyst. Regarding the protonation state of this hydrogen-bonded triad on the axial side of the heme, all our calculations predict a deprotonated acetic acid group (Asp_{235}), in agreement with Siegbahn et al.[24]

Previous work[24] on the quartet spin state of C*c*P Cpd I showed group spin densities distributed over both the heme and the tryptophan residues. We find this to be the case for both the HS and LS spin states. Specifically, the FeO group has two spins indicating two unpaired electrons in π^*_{FeO} orbitals ($\pi^*_{FeO,y}$ and $\pi^*_{FeO,z}$), whereas the third spin is equally distributed over the porphyrin and tryptophan residues. Thus, both spin states in the ground state contain a triradicaloid system with two ferromagnetically coupled electrons in two orthogonal π^*_{FeO} orbitals and a third electron in a mixed porphyrin (a_{2u}) with tryptophan orbital ($a_{2u} + \pi_{Trp}$), and the overall electronic states will have occupation $\pi^*_{FeO,y}{}^1\ \pi^*_{FeO,z}{}^1\ (a_{2u} + \pi_{Trp})^1$ in both the doublet and quartet spin state. In the doublet spin state, the mixed ($a_{2u} + \pi_{Trp}$) orbital is occupied by one electron with β-spin. As a result of the mixing of these two molecular orbitals (a_{2u} and π_{Trp}), the spin densities on the porphyrin and tryptophan groups are $\rho_{Por} = 0.45$ (−0.46) and $\rho_{Trp} = 0.48$ (−0.50) in the HS (LS) spin states.

For small peroxidase model systems it was shown that electronic states with the nonbonding a_{1u} porphyrin orbital singly occupied could be as close as 0.9−1.3 kcal mol^{-1} above the ground state.[25] Therefore, we altered the occupation of the spin states and created the $^{4,2}A_{1u}$ electronic states with occupation $\pi^*_{FeO,y}{}^1\ \pi^*_{FeO,z}{}^1\ a_{2u}{}^2\ a_{1u}{}^1\ \pi_{Trp}{}^2$. These states, however, were found to lie 6.9 ($^4A_{1u}$) and 4.2 ($^2A_{1u}$) kcal mol^{-1} higher in energy than the lowest-lying quartet spin state, so they obviously play a minor role in C*c*P Cpd I. Attempts to swap orbitals to create pure $^{4,2}A_{2u}$ states with occupation $\pi^*_{FeO,y}{}^1\ \pi^*_{FeO,z}{}^1\ a_{2u}{}^1\ a_{1u}{}^2\ \pi_{Trp}{}^2$ or pure $^{4,2}\Pi_{Trp}$ states with occupation $\pi^*_{FeO,y}{}^1\ \pi^*_{FeO,z}{}^1\ a_{2u}{}^2\ a_{1u}{}^2\ \pi_{Trp}{}^1$ failed and converged to the mixed state described above. In all states tested, the spin densities on the imidazole and aspartate groups are negligible.

Therefore, in the gas-phase, the quartet and doublet spin states are virtually degenerate with a slight preference for the quartet spin state. Subsequently, we tested the effect of a dielectric

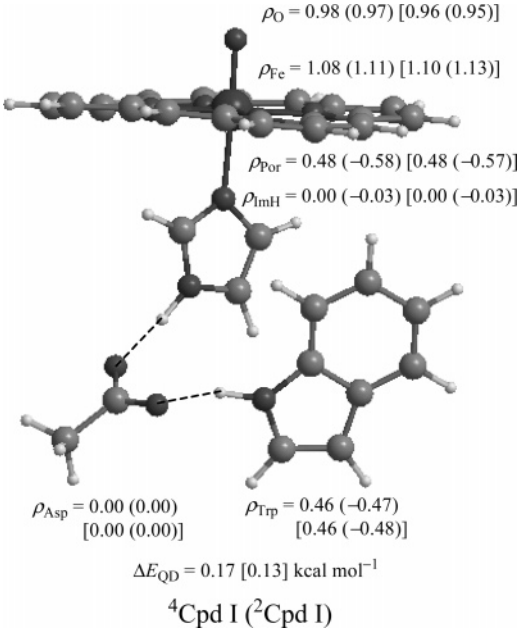

Figure 3. Single point UB3LYP/LACVP calculations with $\epsilon = 5.7$ [$\epsilon = 10.65$] for the lowest quartet (doublet) spin states on optimized UB3LYP/LACVP structures. Also shown is the energy difference between the quartet and doublet states, ΔE_{QD}.

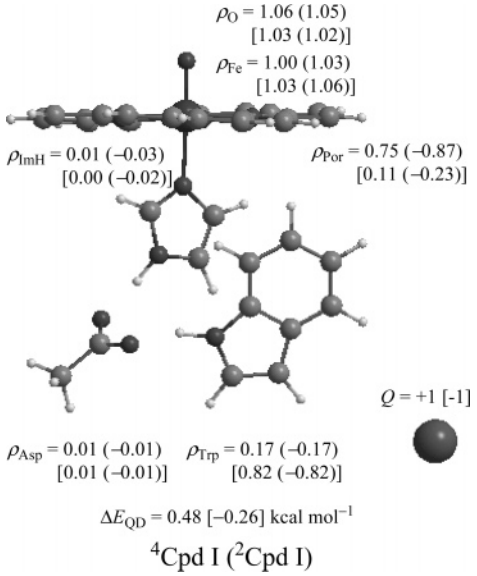

Figure 4. Group spin densities and quartet−doublet energy gap from single point UB3LYP/LACVP calculations on C*c*P Cpd I with an added point charge +1 [−1] to the system.

constant on the relative energies of the spin states and the spin density distributions. We ran single point calculations on the optimized geometries discussed above with a dielectric constant of $\epsilon = 5.7$ and $\epsilon = 10.65$ in order to cover a range of dielectric constants as may be expected in peroxidases, and the results are shown in Figure 3. The addition of a dielectric constant leads to small spin density polarization from the oxygen atom toward the iron. More importantly, the orbital mixing between the porphyrin and tryptophan residues is retained and hardly affected by a dielectric environment. This implies that the tryptophan radical should not be affected by a polar or apolar amino acid environment. The quartet−doublet energy gap stays more or less the same, as well as most group spin densities. Thus, the differences between the active species of C*c*P and APX cannot be explained by differences in a dielectric environment, since otherwise the above results should have shown major differences. The dielectric constant calculations seem to stabilize the $^{4,2}A_{1u}$ states slightly, although the energy gap between the lowest−lying quartet state and the $^4A_{1u}$ state stays above 3.5 kcal mol^{-1}.

Next, we tested the effect of a point charge on the relative energies of the lowest-lying spin states and the spin density distributions. To this end, we added a point charge exactly in the position of the cation binding site in APX as obtained from the X-ray structure[16] and embedded this point charge in the optimized geometries of Figure 2. Subsequently, we carried out single point calculations with a point charge with magnitude $Q = +1$ or -1 in both the quartet and doublet spin states. The obtained spin density distributions and spin state ordering are shown in Figure 4. As can be seen from Figure 4, the point charge hardly affects the electronic situation on the FeO moiety where the spin density stays roughly 2 indicating two singly occupied π^*_{FeO} orbitals. However, a point charge with magnitude $Q = +1$ dramatically changes the third unpaired electron from a mixed porphyrin−tryptophan radical into a porphyrin cation radical leading to spin density of $\rho_{Por} = 0.75$ (HS) and $\rho_{Por} = -0.87$ (LS). The opposite effect occurs with a charge $Q = -1$ applied, whereby the radical moves completely to the tryptophan residue and a spin density of $\rho_{Trp} = 0.82$ (HS) and $\rho_{Trp} = -0.82$ (LS) is obtained. Furthermore, with a point charge with charge $Q = -1$ added the doublet state becomes the ground state, while with a positive charge the quartet state is stabilized over the doublet state. Therefore, the addition of a single point charge at a distance of 8.7 Å away from the tryptophan moiety changes the relative electron affinities of the tryptophan and porphyrin groups as well as the quartet−doublet energy splitting. In particular, a positive charge drives the cation radical character away from the tryptophan to the heme due to charge repulsion between the point charge and the nearby tryptophan group. By contrast, a negatively charged point charge pulls the cation radical to the tryptophan and away from the heme. Our calculations predict that the effect of the point charge of magnitude $Q = +1$ leads to destabilization of the quartet spin state by 7.8 kcal mol^{-1}. This value is in good agreement with Warshel et al.[22] who calculated the effect of the cation binding loop using the Langevin dipole model and estimated the energy contribution to be 6.3 kcal mol^{-1}. The spin density distributions and charges on the aspartate and imidazole groups are hardly affected by the point charges.

Subsequently, we investigated the effect of an applied electric field strength along one of the principal axes of the structure. Previously, we studied the competition of propene C=C epoxidation versus C−H bond hydroxylation using a cytochrome P450 model.[28,29] These calculations showed that the regioselectivity of propene oxidation is strongly dependent on the environment of the catalyst. Thus, in the gas-phase the reaction was predicted to proceed by epoxidation, whereas in a polar environment and the addition of hydrogen bonding as appears in enzymes the regioselectivity changed in favor of hydroxylation. Subsequently, we showed that the addition of an electric field strength along one of the principal axes of the model could change the character of the catalyst, that is, Cpd I, from a porphyrin radical to a thiolate radical.[37] As a result of this, changes in the character of the active species were shown to influence the regioselectivity of epoxidation versus hydroxylation of propene as well. Thus, it was found that the regioselectivity was strongly dependent on the magnitude of the applied electric field as well as its direction. Therefore, we tested the effect of an applied electric field strength along one of the three

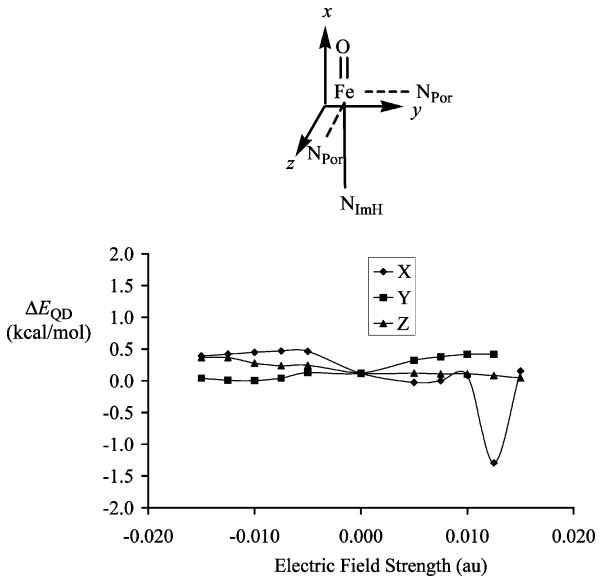

Figure 5. Quartet−doublet energy gap as a function of an applied external electric field along one of the three principal axes. A positive value of ΔE_{QD} reflects a quartet ground state. The location of the coordination system with respect to the central iron−oxo group is shown at the top.

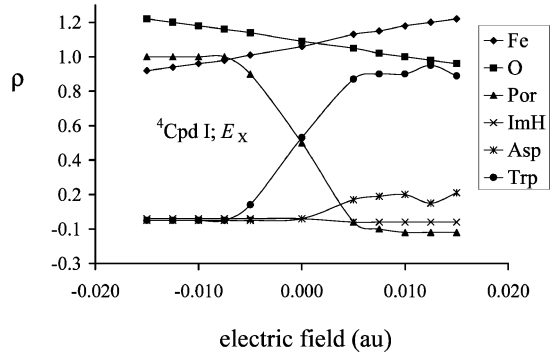

Figure 6. Group spin densities as a function of the applied electric field strength along the molecular *x*-axis for ^{4}Cpd I species. All calculations performed with Gaussian-98 using UB3LYP/LACVP.

principal axes of our C*c*P Cpd I model. Specifically, the *x*-axis is along the Fe−O axis, the *y*-axis is along one of the Fe−N_{Por} distances parallel to the axial ligand, while the *z*-axis is along an orthogonal Fe−N_{Por} distance perpendicular to the axial ligand (see Figure 5). At the bottom of Figure 5 we show the quartet−doublet energy splitting as a function of the electric field strength along each of the three principal axes. As can be seen, an applied electric field strength affects the quartet and doublet spin states differently. Therefore, an electric field strength can alter the quartet−doublet energy gap as well as the quartet−doublet state ordering. Generally, the energy gap between the quartet and doublet states stays within 0.5 kcal mol^{-1}, although it can reach values of up to 1.5 kcal mol^{-1}. The strongest effects are obtained with a field along the *x*-axis which is along the Fe−O axis and perpendicular to the plane of the porphyrin. Since, the a_{2u} molecular orbital is a nonbonding π-orbital of the porphyrin, it is exactly in this plane that the a_{2u} molecular orbital is located, so that the effects are the most efficient there. Therefore, local effects such as an applied electric field strength of the protein on the active site of the enzyme can change the nature of the electronic state from a quartet to a doublet spin state and vice versa.

In Figure 6 we show the group spin densities of ^{4}Cpd I as a function of an applied electric field strength along the *x*-axis. Similar results are obtained for an applied electric field along the *y*- or *z*-axis, as well as for ^{2}Cpd I, see Supporting Information. Some interesting features can be seen from Figure 6. First, the spin densities of the FeO moieties add up to approximately 2, but their individual values change with the nature of the field strength. In particular, in positive fields the spin densities of the FeO moiety are polarized toward the iron atom with spin densities of $\rho_{Fe} = 1.17$ and $\rho_O = 0.91$ using a field $E_{field} = 0.015$ au. By contrast, using an electric field of opposite direction ($E_{field} = -0.015$ au) spin densities of $\rho_{Fe} = 0.87$ and $\rho_O = 1.17$ are obtained, which is almost a complete reversal from the field in the positive direction. Since the charge of the oxygen atom is dependent on the spin density, the catalytic properties of the iron−oxo system may be influenced by electric field effects as a more negatively charged oxygen atom, for instance, will more easily abstract a proton from a substrate. Thus, an electric field effect as induced by the protein backbone on the active center of the enzyme influences the FeO charge distribution and thereby the catalytic properties of the iron−oxo center.

Other effects visible in Figure 6 are the accumulation of some spin density (of up to $\rho_{Asp} = 0.20$) on the aspartic acid residue with a positive electric field applied. This changes the anionic character of this group to more radical character and may weaken the hydrogen bonds toward the aspartate group. It may further result in reorientation of the protonation state of the hydrogen-bonded triad on the axial site of the enzyme.

The most striking point shown in Figure 6, however, is the sharp differences in spin density on the porphyrin and tryptophan groups. Initially, in the gas-phase without applied electric field ($E_{field} = 0$) almost identical group spin densities on porphyrin and tryptophan are obtained (Figure 2 above), but with an electric field ($E_{field} = 0.015$ au) applied along the positive *x*-axis the spin densities move completely to the tryptophan ($\rho_{Trp} = 0.84$) and at the same time the spin density on the porphyrin reduces to almost zero. By contrast, in a field with opposite direction ($E_{field} = -0.015$ au), the reverse happens and spin density accumulates on the porphyrin ($\rho_{Por} = 0.95$) while it reduces strongly on the tryptophan. Thus, whereas the system in the gas phase has a mixed porphyrin−tryptophan orbital ($a_{2u} + \pi_{Trp}$) with single occupancy, with an electric field applied along the negative *x*-axis the electronic state changes to a pure porphyrin type orbital (a_{2u}), while pointing in the opposite direction it generates a pure tryptophan orbital (π_{Trp}). Therefore, the nature of the electronic state and the location of the radical in C*c*P is strongly dependent on environmental effects, such that a simple point charge or an applied electric field strength can change the location of the radical and consequently change the nature of the catalytic properties of the enzyme.

Discussion

In this work we presented results on the quartet−doublet energy splitting and the electronic properties of the ground state of Cpd I of a C*c*P model. Thus, since heme enzymes contain close-lying doublet and quartet spin states, the general reactivity pattern is via two-state reactivity (TSR)[26] whereby different reaction mechanisms on the separate surfaces can compete. It was shown, for instance, that side reactions during alkene epoxidations, such as rearrangements to form aldehydes or the formation of suicidal complexes, occur only on the quartet spin surface.[27] Therefore, the doublet−quartet energy splitting is an important feature of the enzyme which decides the substrate specificity and product distributions.

Generally, the system can exist in two different electronic situations, namely, with a porphyrin hole and a closed-shell

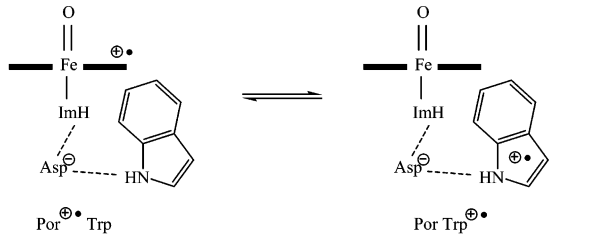

	(*i*)	(*ii*)	(*iii*)	(*iv*)	(*v*)	(*vi*)	(*vii*)
	ε = 1	ε = 5.7	ε = 10.65	ε = 1; Q = 1	ε = 1; Q = -1	ε = 1 E_x = 0.015	ε = 1 E_x = -0.015
ρ_{FeO}	2.05	2.06	2.06	2.06	2.06	2.08	2.04
ρ_{Por}	0.45	0.48	0.48	0.75	0.17	-0.07	0.95
ρ_{Trp}	0.48	0.46	0.46	0.11	0.82	0.84	0.00
ΔE_{QD}	0.12	0.17	0.13	0.48	-0.26	0.39	-0.15
	Mixed States			Por$^{\oplus\bullet}$ Trp	Por Trp$^{\oplus\bullet}$	Por Trp$^{\oplus\bullet}$	Por$^{\oplus\bullet}$ Trp

Figure 7. The different electronic configurations of C*c*P Cpd I (top) and the group spin densities of the FeO, porphyrin, and indole groups and the quartet−doublet energy splitting (in kcal mol^{-1}) under various environmental conditions. A positive quartet−doublet energy means a quartet spin ground state. From left to right the perturbations include (i) optimized geometry in the gas-phase ($\epsilon = 1$), (ii) single point in a dielectric constant with $\epsilon = 5.7$, (iii) single point calculation in a dielectric constant with $\epsilon = 10.65$, (iv) single point calculation with a point charge of $Q = +1$, (v) single point calculation with a point charge of $Q = -1$, (*vi*) single point calculation with an electric field of magnitude $E_{field} = 0.015$ au along the *x*-axis, and (vii) single point calculation with an electric field of magnitude $E_{field} = -0.015$ au along the *x*-axis.

tryptophan group (Por$^{+\bullet}$ Trp) or with a cation radical situation located on the tryptophan and a closed-shell porphyrin (Por Trp$^{+\bullet}$), Figure 7 (top). Electronically, the Por$^{+\bullet}$ Trp state corresponds to an electronic state with $\pi^*_{FeO,y}{}^1\,\pi^*_{FeO,z}{}^1\,a_{2u}{}^1\,\pi_{Trp}{}^2$ configuration, while the Por Trp$^{+\bullet}$ state corresponds to a $\pi^*_{FeO,y}{}^1\,\pi^*_{FeO,z}{}^1\,a_{2u}{}^2\,\pi_{Trp}{}^1$ configuration. In the gas-phase calculations, however, these two states mix and an electronic state with partial cation radical on both porphyrin and tryptophan groups is obtained with spin densities $\rho_{Por} = 0.48$ and $\rho_{Trp} = 0.48$ in the quartet spin state. This charge and spin delocalization is the result from comparable electron affinities between the tryptophan and porphyrin groups in the gas phase. For an isolated porphyrin group ($PorH_2$) we calculated an electron affinity of 6.71 eV, while for an isolated indole (IndH) a value of 7.56 eV is obtained at the B3LYP/6-311+G* level of theory. However, environmental interactions, such as the hydrogen bond from Asp_{235} to indole, may influence the electron affinity so that it is lowered and becomes competitive with the porphyrin group. Indeed, small external perturbations influence the electron affinity of the indole and porphyrin groups, so that the electronic state of C*c*P Cpd I varies under different environmental conditions. Figure 7 summarizes the spin density contributions of the FeO, porphyrin, and tryptophan groups for the quartet spin state of C*c*P Cpd I as well as the quartet−doublet energy splitting (ΔE_{QD}) under different environmental conditions. The results for the doublet state are analogous and not shown. The addition of a dielectric constant to the model gives minor changes in spin densities and quartet−doublet energy splittings and keeps the mixed character of the ground state. However, a single point charge at 8.7 Å from the active center influences the ground-state properties and quartet−doublet energy splittings considerably. In particular, a point charge with $Q = +1$ creates a Por$^{+\bullet}$ Trp state, whereas a point charge in the opposite direction generates a Por Trp$^{+\bullet}$ state. This implies that indeed a cation binding loop as has been observed in APX systems influences the nature of the cation radical in the Cpd I state and thereby creates a different electronic situation as appears in C*c*P Cpd I. This effect can also be induced by an electric field strength along one of the principal axes of the active center. For instance, an applied electric field strength along the *x*-axis, that is, along the FeO bond, has an effect similar to that of the addition of a point charge in a sense that either a pure porphyrin cation radical or a pure tryptophan radical is created. It should be emphasized that the quartet−doublet splitting is influenced differently; for instance, in Figure 7 we show two ways to create a porphyrin cation radical state. In one case, the quartet spin state is stabilized with the addition of a point charge of $Q = +1$, while in another the addition of an electric field strength along the negative *x*-axis is seen to stabilize the doublet spin state instead more strongly. As a result of this, the point charge calculation gives a quartet ground state, whereas the electric field calculation gives a doublet ground state. Therefore, this shows that the differences between the active species of C*c*P and APX Cpd I are determined by small environmental perturbations, such as the cation binding loop and also by the electric field strength as applied by the protein. These factors do not necessarily contribute equally and additively.

One of the criteria for the enzyme to be a good and efficient catalyst is its capability to accept electrons efficiently. Thus, HRP functions as an electron sink and has a high electron affinity (EA) of 6.41 eV.[25] In the case of C*c*P Cpd I, we calculate an electron affinity of 4.11 eV for the quartet spin state at the LACV3P+* level of theory, while this value increases to 5.17 eV in a dielectric constant of $\epsilon = 5.7$ and to 5.30 eV in a dielectric constant of $\epsilon = 10.65$. Therefore, the EA of C*c*P is significantly lower than the one obtained for an HRP Cpd I model, mainly as a result of the mixing of the porphyrin and tryptophan molecular orbitals, Figure 7. Similar results were obtained for cytochrome P450 models, which showed that the axial thiolate ligand mixes with the porphyrin a_{2u} orbital, thereby decreasing the electron affinity of Cpd I significantly to 3.06 eV.[40,41] Since the interactions in C*c*P Cpd I between the a_{2u} and π_{Trp} orbitals are much less than between the a_{2u} and π_S orbitals in P450, the electron affinity is higher in C*c*P.

On the basis of these results we can make some predictions regarding the reactivity of the enzyme C*c*P with respect to typical substrates, assuming that the model mimics the enzyme sufficiently and that substrate bonding and the accessibility of the substrate to the pocket are not hampered within the enzyme environment. First, the electron affinity of Cpd I is much smaller than the one obtained by HRP, but it is not as small as the one obtained for P450. This means that C*c*P Cpd I is less suitable as an electron sink than HRP. Furthermore, its reactivity pattern will likely be somewhere midway between the ones observed for P450 and HRP enzymes. A recent study on the comparisons between propene epoxidation versus propene hydroxylation with an HRP model Cpd I and a P450 model Cpd I showed marked differences.[29,42] First, the reaction barriers with the HRP model were significantly lower than the ones obtained with a P450 model and mainly as a result of the difference in electron affinity between HRP and P450 enzymes. Due to the fact that C*c*P contains a tryptophan radical rather than a heme radical, it means that the electron affinity is reduced with respect to HRP but not as much as in P450 enzymes, which means that C*c*P is between these two extremes.

Figure 8a shows the epoxidation reaction mechanism of a heme enzyme with a substrate (propene in this case), whereby

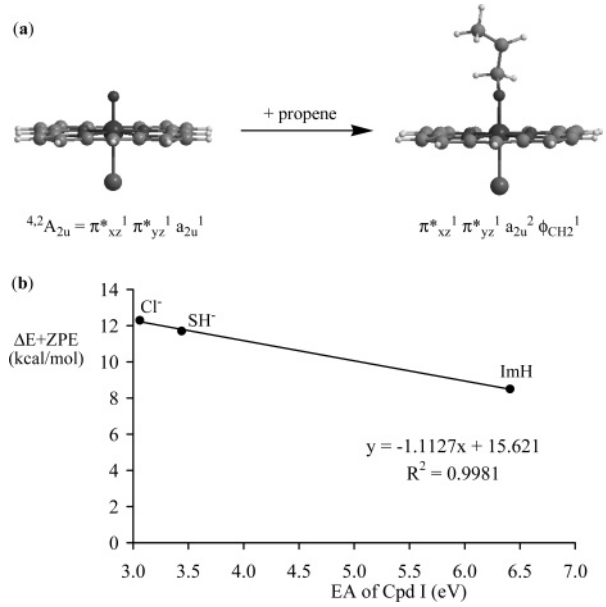

Figure 8. (a) General reaction mechanism for the C−O bond activation step in the epoxidation of propene by oxo−iron porphyrins and the corresponding orbital occupation of reactant and product. (b) Doublet spin barrier heights (ΔE + ZPE) for oxo−iron porphyrin systems with chloride, thiolate, or imidazole ligands as a function of the electron affinity of Cpd I. Energies are obtained at the UB3LYP/ LACV3P+* with UB3LYP/LACVP level ZPE corrections from refs 27e,29,43.

an initial C−O bond activation step leads to a radical intermediate that later rearranges to form the epoxide (not shown). We have calculated this reaction using several oxo−iron porphyrin systems with various axial ligands, namely thiolate (SH^-), imidazole (ImH), and chloride (Cl^-).[27e,29,43] All these Cpd I complexes have a ground state with close-lying doublet and quartet spin states with orbital occupation $\pi^*_{xz}{}^1$ $\pi^*_{yz}{}^1$ $a_{2u}{}^1$ ($^{4,2}A_{2u}$). The C−O bond activation of propene in all cases leads to a radical intermediate with orbital occupation $\pi^*_{xz}{}^1$ $\pi^*_{yz}{}^1$ $a_{2u}{}^2$ $\phi_{CH2}{}^1$. Thus, the initial step in the epoxidation mechanism is accomplished by electron transfer from the substrate into the a_{2u} orbital and formation of a C−O bond. Therefore, the C−O bond activation barrier may be dependent, albeit partially, on the electron affinity of the a_{2u} orbital in Cpd I. To test this hypothesis, in Figure 8b, we show the correlation between the C−O activation barrier for propene epoxidation and the electron affinity of the reactant for the doublet spin state with chloride, thiolate, or imidazole axial ligands. Although, the trend contains only three data points, there seems to be a good correlation. If this correlation holds for C*c*P Cpd I as well, this implies that the epoxidation barrier of propene will be midway between the one obtained for Cpd I with imidazole and thiolate as axial ligand, since C*c*P Cpd I has an electron affinity of 4.11 eV. Nevertheless, it should be pointed out that other factors, such as the size of the enzyme pocket as well as the electrostatic interactions within the pocket which influence substrate binding, may change the ordering as described here.

Conclusions

DFT calculations on the active site model of C*c*P Cpd I have been performed. Calculations show that the quartet−doublet energy splitting is strongly dependent on local perturbations. In particular, a point charge 8.7 Å away from the tryptophan radical can change the system from a mixed porphyrin−tryptophan radical into a pure porphyrin or tryptophan radical dependent on the direction of the point charge. In addition, an applied electric field strength along one of the principal axes of the active species can change the system into a pure porphyrin radical or a pure tryptophan radical. Moreover, these perturbations give varying quartet−doublet energy splittings, which eventually may influence the reactivity of the enzyme. Effects of the quartet−doublet energy splitting on the activity of C*c*P Cpd I and its reactivity patterns are analyzed.

Acknowledgment. The research was supported by CPU time provided by the Computational Chemistry Working Party (CCWP) and the University of Manchester.

Supporting Information Available: Six tables with relative energies, group spin densities, and charges of various Cpd I structures under different environmental conditions. Also provided are eleven figures with structural data and effects of an electric field on energies and group spin densities. This material is available free of charge via the Internet at http://pubs.acs.org.

References and Notes

(1) *The Porphyrin Handbook*; Kadish, K. M., Smith, K. M., Guilard, R., Eds.; Academic Press: San Diego, CA, 2000.
(2) Cytochrome P450: *Structure, Mechanism and Biochemistry*, 3rd ed.; Ortiz de Montellano, P. R., Ed.; Kluwer Academic/Plenum Publishers: New York, 2004.
(3) Finzel, B. C.; Poulos, T. L.; Kraut, J. *J. Biol. Chem.* **1984**, *259*, 13027−13036.
(4) Ortiz de Montellano, P. R. *Annu. Rev. Pharmacol. Toxicol.* **1992**, *32*, 89−107.
(5) Fülöp, V.; Watmough, N. J.; Ferguson, S. J. *Adv. Inorg. Chem.* **2001**, *51*, 163−204.
(6) Goodin, D. B.; McRee, D. E. *Biochemistry* **1993**, *32*, 3313−3324.
(7) Berglund, G. I.; Carlsson, G. H.; Smith, A. T.; Szöke, H.; Henriksen, A.; Hajdu, J. *Nature* **2002**, *417*, 463−468.
(8) Green, M. T.; Dawson, J. H.; Gray, H. B. *Science* **2004**, *304*, 1653−1656.
(9) Poulos, T. L. *J. Bioinorg. Chem.* **1996**, *1*, 356−359.
(10) Ogliaro, F.; de Visser, S. P.; Shaik, S. *J. Inorg. Biochem.* **2002**, *91*, 554−567.
(11) Shimizu, H.; Schuller, D. J.; Lanzilotta, W. N.; Sundaramoorthy, M.; Arciero, D. M.; Hooper, A. B.; Poulos, T. L. *Biochemistry* **2001**, *40*, 13483−13490.
(12) Green, M. T. *J. Am. Chem. Soc.* **2000**, *122*, 9495−9499.
(13) Harris, D. L. *Curr. Opin. Chem. Biol.* **2001**, *5*, 724−735.
(14) Sivaraja, M.; Goodin, D. B.; Smith, M.; Hoffman, B. M. *Science* **1989**, *245*, 738−740.
(15) Huyett, J. E.; Doan, P. E.; Gurbiel, R.; Houseman, A. L. P.; Sivaraja, M.; Goodin, D. B.; Hoffman, B. M. *J. Am. Chem. Soc.* **1995**, *117*, 9033−9041.
(16) Sharp, K. H.; Mewies, M.; Moody, P. C. E.; Raven, E. L. *Nat. Struct. Biol.* **2003**, *10*, 303−307.
(17) Raven, E. L. *Nat. Prod. Rep.* **2003**, *20*, 367−381.
(18) Berman, H. M.; Westbrook, J.; Feng, Z.; Gilliland, G.; Bhat, T. N.; Weissig, H.; Shindyalov, I. N.; Bourne, P. E. *Nucleic Acids Res.* **2000**, *28*, 235−242.
(19) Bhaskar, B.; Bonagura, C. A.; Li, H.; Poulos, T. L. *Biochemistry* **2002**, *41*, 2684−2693.
(20) Hirst, J.; Wilcox, S. K.; Williams, P. A.; Blankenship, J.; McRee, D. E.; Goodin, D. B. *Biochemistry* **2001**, *40*, 1265−1273.
(21) Hirst, J.; Wilcox, S. K.; Ai, J.; Moënne-Loccoz, P.; Loehr, T. M.; Goodin, D. B. *Biochemistry* **2001**, *40*, 1274−1283.
(22) Jensen, G. M.; Bunte, S. W.; Warshel, A.; Goodin, D. B. *J. Phys. Chem. B* **1998**, *102*, 8221−8228.
(23) Menyhárd, D. K.; Náray-Szabó, G. *J. Phys. Chem. B* **1999**, *103*, 227−233.
(24) Wirstam, M.; Blomberg, M. R. A.; Siegbahn, P. E. M. *J. Am. Chem. Soc.* **1999**, *121*, 10178−10185.
(25) de Visser, S. P.; Shaik, S.; Sharma, P. K.; Kumar, D.; Thiel, W. *J. Am. Chem. Soc.* **2003**, *125*, 15779−15788.
(26) Shaik, S.; de Visser, S. P.; Ogliaro, F.; Schwarz, H.; Schröder, D. *Curr. Opin. Chem. Biol.* **2002**, *6*, 556−567.
(27) (a) de Visser, S. P.; Ogliaro, F.; Harris, N.; Shaik, S. *J. Am. Chem. Soc.* **2001**, *123*, 3037−3047. (b) de Visser, S. P.; Ogliaro, F.; Shaik, S. *Angew. Chem., Int. Ed.* **2001**, *40*, 2871−2874. (c) de Visser, S. P.; Ogliaro, F.; Shaik, S. *Chem. Commun.* **2001**, 2322−2323. (d) de Visser, S. P.; Kumar, D.; Shaik, S. *J. Inorg. Biochem.* **2004**, *98*, 1183−1193. (e) Kumar, D.; de Visser, S. P.; Shaik, S. *Chem. Eur. J.* **2005**, *11*, 2825−2835.

(28) de Visser, S. P.; Ogliaro, F.; Sharma, P. K.; Shaik, S. *Angew. Chem., Int. Ed.* **2002**, *41*, 1947−1951

(29) de Visser, S. P.; Ogliaro, F.; Sharma, P. K.; Shaik, S. *J. Am. Chem. Soc.* **2002**, *124*, 11809−11826.

(30) (a) Kumar, D.; de Visser, S. P.; Shaik, S. *J. Am. Chem. Soc.* **2003**, *125*, 13024−13025. (b) Kumar, D.; de Visser, S. P.; Sharma, P. K.; Cohen, S.; Shaik, S. *J. Am. Chem. Soc.* **2004**, *126*, 1907−1920. (c) Kumar, D.; de Visser, S. P.; Shaik, S. *J. Am. Chem. Soc.* **2004**, *126*, 5072−5073.

(31) (a) de Visser, S. P.; Shaik, S. *J. Am. Chem. Soc.* **2003**, *125*, 7413−7424. (b) Sharma, P. K.; de Visser, S. P.; Shaik, S. *J. Am. Chem. Soc.* **2003**, *125*, 8698−8699. (c) Kumar, D.; de Visser, S. P.; Sharma, P. K.; Hirao, H.; Shaik, S. *Biochemistry* **2005**, *44*, 8148−8158.

(32) *Jaguar 5.5*; Schrödinger, Inc.: Portland, OR, 2000.

(33) Becke, A. D. *J. Chem. Phys.* **1993**, *98*, 5648−5652.

(34) Lee, C.; Yang, W.; Parr, R. G. *Phys. Rev. B* **1988**, *37*, 785−789.

(35) Hay, J. P.; Wadt, W. R. *J. Chem. Phys.* **1985**, *82*, 270−283.

(36) *Gaussian 98*, Revision A.7; Frisch, M. J.; Trucks, G. W.; Schlegel, H. B.; Scuseria, G. E.; Robb, M. A.; Cheeseman, J. R.; Zakrzewski, V. G.; Montgomery, J. A., Jr.; Stratmann, R. E.; Burant, J. C.; Dapprich, S.; Millam, J. M.; Daniels, A. D.; Kudin, K. N.; Strain, M. C.; Farkas, O.; Tomasi, J.; Barone, V.; Cossi, M.; Cammi, R.; Mennucci, B.; Pomelli, C.; Adamo, C.; Clifford, S.; Ochterski, J.; Petersson, G. A.; Ayala, P. Y.; Cui, Q.; Morokuma, K.; Malick, D. K.; Rabuck, A. D.; Raghavachari, K.; Foresman, J. B.; Cioslowski, J.; Ortiz, J. V.; Baboul, A. G.; Stefanov, B. B.; Liu, G.; Liashenko, A.; Piskorz, P.; Komaromi, I.; Gomperts, R.; Martin, R. L.; Fox, D. J.; Keith, T.; Al-Laham, M. A.; Peng, C. Y.; Nanayakkara, A.; Gonzalez, C.; Challacombe, M.; Gill, P. M. W.; Johnson, B.; Chen, W.; Wong, M. W.; Andres, J. L.; Gonzalez, C.; Head-Gordon, M.; Replogle, E. S.; Pople, J. A. Gaussian Inc.: Pittsburgh, PA, 1998.

(37) Shaik, S.; de Visser, S. P.; Kumar, D. *J. Am. Chem. Soc.* **2004**, *126*, 11746−11749.

(38) Chance, M.; Powers, L.; Poulos, T. L.; Chance, B. *Biochemistry* **1986**, *25*, 1266−1270.

(39) Bonagura, C. A.; Bhaskar, B.; Shimizu, H.; Li, H.; Sundaramoorthy, M.; McRee, D. E.; Goodin, D. B.; Poulos, T. L. *Biochemistry* **2003**, *42*, 5600−5608.

(40) Ogliaro, F.; Cohen, S.; de Visser, S. P.; Shaik, S. *J. Am. Chem. Soc.* **2000**, *122*, 12892−12893.

(41) Ogliaro, F.; de Visser, S. P.; Cohen, S.; Kaneti, J.; Shaik, S. *ChemBioChem* **2001**, 848−851.

(42) Kumar, D.; de Visser, S. P.; Sharma, P. K.; Derat, E.; Shaik, S. *J. Biol. Inorg. Chem.* **2005**, *10*, 181−189.

(43) de Visser, S. P. *J. Biol. Inorg. Chem.*, accepted for publication.